Electronic structure of tetraphenyldithiapyranylidene: A valence effective Hamiltonian theoretical investigation

R. Viruela-Martín, P. M. Viruela-Martín, and E. Ortí[a)]
Departamento de Química-Física, Universitat de València, Dr. Moliner 50, E-46100 Burjassot, Spain

(Received 24 September 1991; accepted 5 December 1991)

We present a theoretical investigation of the electronic structure of tetraphenyldithiapyranylidene ($DIPS\Phi_4$) using the nonempirical valence effective Hamiltonian (VEH) method. Molecular geometries are optimized at the semiempirical PM3 level which predicts an alternating nonaromatic structure for the dithiapyranylidene (DIPS) framework. The VEH one-electron energy level distribution calculated for $DIPS\Phi_4$ is presented as a theoretical XPS simulation and is analyzed by comparison to the electronic structure of its molecular components DIPS and benzene. The theoretical VEH spectrum is found to be fully consistent with the experimental solid-state x-ray photoelectron spectroscopy (XPS) spectrum and an excellent quantitative agreement between theory and experiment is achieved when comparing the energies of the main peaks. A detailed interpretation of all the experimental photoemission bands is reported in the light of the VEH results.

I. INTRODUCTION

In recent works,[1–3] we presented detailed discussions of the electronic structure of metal-free phthalocyanine (H_2Pc) (Refs. 1, 2) and metal-free porphine (H_2P) (Ref. 3) molecules on the basis of valence effective Hamiltonian (VEH) calculations. The calculated VEH density of valence states was found to be in excellent quantitative agreement with experimental photoemission data. This allowed us to provide a full interpretation of the gas-phase and solid-state photoelectron spectra of metal-free phthalocyanine and porphine molecules.

In this work, we focus on an investigation of the valence electronic structure of the tetraphenyldithiapyranylidene molecule, named hereafter as $DIPS\Phi_4$, (Fig. 1). The electronic structure of the parent dithiapyranylidene molecule (DIPS) is also studied as a reference point. Our interest in these molecular systems results from the fact that both DIPS and $DIPS\Phi_4$ are useful precursors of organic one-dimensional conductors. DIPS is a 14 π-electron system, as the extensively studied π-donor tetrathiafulvalene (TTF), and reacts with the acceptor 7,7,8,8-tetracyanoquinodimethane (TCNQ) to give a variety of charge-transfer salts with different stoichiometries.[4–6] $DIPS\Phi_4$ gives rise to a wider range of highly conducting compounds, since it forms charge-transfer complexes with TCNQ,[7,8] mixed valence radical-cation salts obtained by oxidation with iodine,[9–11] and diamagnetic dication salts-type $DIPS\Phi_4^{2+}\cdot 2X$ ($X = PF_6^-, ClO_4^-$).[12] $DIPS\Phi_4$ has been also used as a weak n-dopant of phthalocyanines[13,14] and its 1:1 adduct with the acceptor nickel (II)-*bis*(1,3-dithiole-2-thione-4,5,dithiolate) $[Ni(dmit)_2]^{2-}$ has been recently reported.[15] The main difference between $DIPS\Phi_4$ and DIPS is that, oppositely to TTF, the presence of phenyl substituents in $DIPS\Phi_4$ favors the formation of radical-cation salts and charge-transfer complexes which exhibit metallic conductivity (250–300 S/cm at room temperature).[7–11] On the contrary, DIPS only gives rise to semiconducting materials.[4–6] A great variety of conducting compounds has been also obtained from other (pyranyl)pyrans including selenium and tellerium analogues of $DIPS\Phi_4$.[16–19]

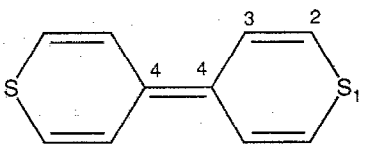

DIPS

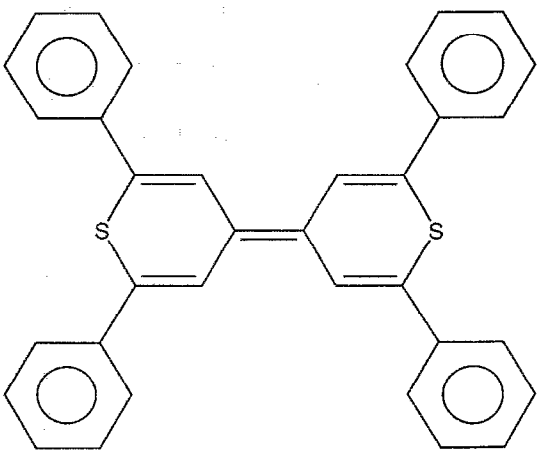

$DIPS\Phi_4$

FIG. 1. Molecular structure and labeling of dithiapyranylidene (DIPS) and tetraphenyldithiapyranylidene ($DIPS\Phi_4$).

[a)] Author to whom correspondence should be addressed.

 0021-9606/92/064474-10$06.00

The valence electronic structure of DIPSΦ_4 has been experimentally investigated using the x-ray photoelectron spectroscopy (XPS) technique.[20,21] Boutique *et al.*[20] reported the solid-state XPS spectra of neutral DIPSΦ_4, several of its polyiodides and the DIPS$\Phi_4^{2+} \cdot 2ClO_4^-$ salt. El-Khatib *et al.*[21] reinvestigated the spectrum of the neutral compound using the same photon energy (Al Kα radiation). These authors also performed theoretical calculations by means of the approximated MSXα method in order to interpret the XPS spectrum of DIPSΦ_4.[21,22] More accurate minimal STO-3G basis set *ab initio* calculations had been previously reported by Boutique *et al.*[23] on the DIPS molecule, used as a simplified model to study the electronic-structure characteristics of DIPSΦ_4.

The purpose of this paper is to perform a comprehensive theoretical analysis of the whole valence electronic structure of DIPSΦ_4 using DIPS as a reference point. As in the case of metal-free phthalocyanine and porphine,[1-3] we wish to provide a detailed interpretation of the available XPS spectra of DIPSΦ_4. The large size and complexity of DIPSΦ_4, $C_{34}H_{24}S_2$ (260 total electrons, 172 valence electrons), makes rather difficult to apply standard *ab initio* methods to calculate its electronic structure. In this work, we use the totally nonempirical valence effective Hamiltonian (VEH) pseudopotential method. The validity of the VEH approach to study the electronic structure of large π-electronic molecular systems has been widely illustrated in previous works.[1-3,24,25]

II. COMPUTATIONAL DETAILS

The VEH quantum-chemical technique has been extensively described elsewhere.[26-28] It takes only into account the valence electrons and is parametrized to reproduce the results of *ab initio* Hartree–Fock calculations without performing any self-consistent-field (SCF) process or calculating any bielectronic integral. The VEH method therefore is an especially useful tool to deal with large molecular or crystalline systems, since it yields one-electron energies of *ab initio* double-zeta quality at a reasonable computer cost. The VEH calculations have been performed using the atomic potentials previously optimized for hydrogen, carbon, and sulfur.[28-30]

In order to obtain a theoretical simulation of the photoemission (UPS or XPS) spectra, the one-electronic molecular energy levels ϵ_i are convoluted by Gaussian functions of adjustable full width at the half-maximum (FWHM) as explained in Ref. 1. Furthermore, the intensity of each Gaussian function is modulated for the XPS spectra by an additional factor α_i. This factor takes into account the different experimental photoemission cross sections σ_p of the atomic orbitals involved in each molecular level and is calculated using the model of Gelius.[31] The values used for σ_p are the following:[31] $\sigma(S,3s) = 0.47$, $\sigma(S,3p) = 0.47/1.1$, $\sigma(C,2s) = 1$, $\sigma(C,2p) = 1/13$, and $\sigma(H,1s) = 0$; $\sigma(C,2s)$ is being taken as a reference.

The molecular geometries used for DIPS and DIPSΦ_4 in the VEH calculations have been obtained from theoretical optimizations using *ab initio* and semiempirical Hartree–Fock methods. The most stable conformation of DIPS has been calculated at the STO-3G* *ab initio* level using the MONSTERGAUSS system of programs.[32] We have employed the STO-3G* basis set which includes polarization *d* orbitals on the sulfur atoms since this is a necessary requirement to obtain meaningful bond lengths and bond angles in molecules involving sulfur atoms.[33] The geometry of DIPS has been also optimized by means of the MNDO-PM3 (modified neglect of diatomic overlap, parametric method number 3) semiempirical method[34] as implemented in the MOPAC-6.0 system of programs.[35] The MNDO-PM3 method represents an improved version of the first two MNDO-type methods, MNDO (Ref. 36) and AM1 (Austin Model 1), (Ref. 37) since it corresponds to a reparameterization of the MNDO approach in which the AM1 form of the core–core interaction is used.[34] The large size of the DIPSΦ_4 molecule prevents any geometrical optimization at *ab initio* level and it has only been optimized using the PM3 method.

III. RESULTS AND DISCUSSION

A. Geometrical considerations

The optimized geometries obtained for the DIPS molecule at the STO-3G*-*ab initio* and PM3-semiempirical levels are depicted in Fig. 2(a). In a first approach, both geometries have been calculated assuming that the molecule is totally planar and has D_{2h} symmetry. However, since x-ray diffraction data on neutral DIPSΦ_4 (Ref. 38) indicate that the thiapyranylidene rings are only approximately planar showing some tendency to have boatlike conformations, we have also performed STO-3G* and PM3 optimizations starting from geometries distorted from planarity. It is to be noted that all of these calculations lead to the same planar geometries displayed in Fig. 2(a) for DIPS and confirm the D_{2h} planar structure as a minimum. This result contrasts with the solid-state data reported for DIPSΦ_4 (Ref. 38), but is in perfect agreement with the gas-phase microwave structures obtained for the related 4*H*-thiapyran-4-one and 4*H*-thiapyran-4-thione compounds,[39] for which the thiapyranylidene ring is observed to be totally planar.

As can be seen in Fig. 2(a), the molecular structures calculated for DIPS are highly localized and suggest that the molecule is essentially nonaromatic. At the PM3 level, the C2–C3 distance is calculated to have a value of 1.342 Å, which clearly corresponds to a formal double bond since it is only slightly longer than the standard double bond of ethylene (1.339 Å).[40] The central C4–C4′ bond also corresponds essentially to a double bond since it is predicted to have a length of 1.375 Å. The formal C3–C4 single bonds (1.457 Å) show some π-conjugation between the adjacent C4–C4′ and C2–C3 double bonds and are a little shorter than the corresponding bond in nonaromatic cyclopentadiene.[41] These results contrast with the molecular structure of biphenyl, the all-carbon analog of DIPS, where basically two aromatic benzene rings (all C–C bond distances are about 1.38–1.40 Å) are linked by a single C–C bond ($\approx$1.50 Å).[42-44] The substitution of two C–H units in biphenyl by two sulphur atoms to obtain the DIPS molecule implies the introduction of two extra π-electrons passing from a 12π- to a 14π-electron system which produces the loss of aromatic character.

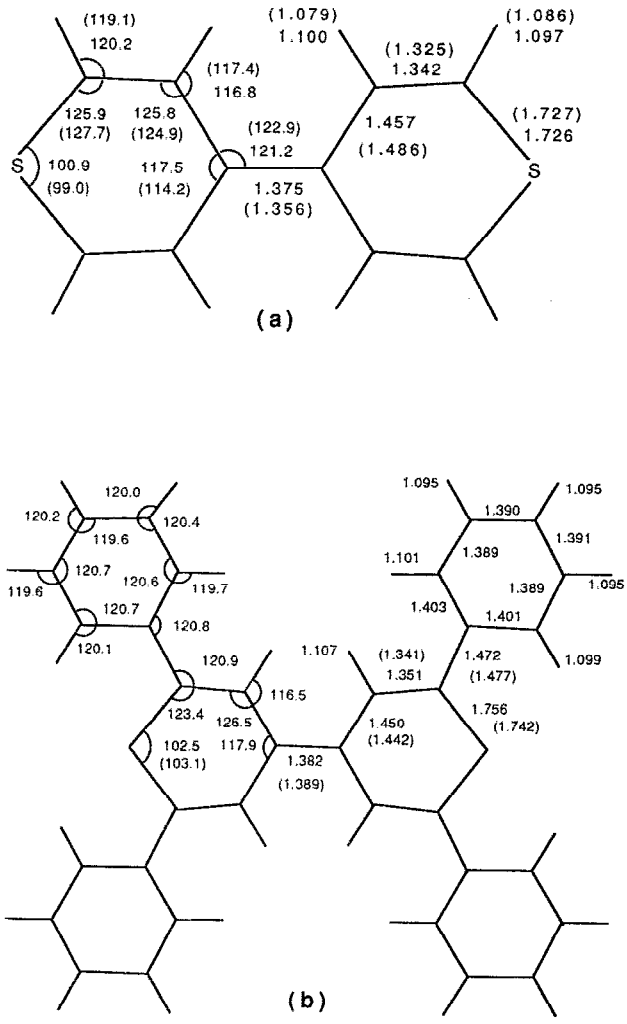

FIG. 2. (a) PM3-optimized geometry for DIPS, (STO-3G* optimized parameters are included in parentheses); (b) PM3-optimized geometry for DIPSΦ_4, (x-ray solid-state data from Ref. 38 are included in parentheses for the most relevant parameters). Bonds are in Å and angles in degrees. D_{2h} planar geometries have been assumed for both molecules.

Furthermore, the introduction of sulphur atoms causes large angular distortions, all the bond angles largely deviate from regular 120° hexagonal angles. The calculated C–S bond distance (1.726 Å) is very similar to that observed for thiophene (1.714 Å), but the C–S–C bond angle (100.9°) is considerably larger than in thiophene (92.1°).[45]

The optimized geometric parameters calculated for the DIPS molecule at the STO-3G* level are very similar to those obtained at the PM3 level [see Fig. 2(a)] and show identical trends to those discussed above. Comparing to the PM3 results, the STO-3G* basis set seems to provide too short double bonds and too long single C–C bonds. The reliability of both approaches is discussed below by comparing to experimental data on DIPSΦ_4.[38] The geometrical structure of DIPS has been also optimized using the MNDO[36] and AM1[37] methods in order to compare with the results obtained with the more recent PM3 approach. In agreement with previous reported data,[46,47] both the MNDO and AM1 methods provide too short C–S bond lengths (1.647 and 1.666 Å, respectively).

Experimental structural data are only available for several DIPS-TCNQ charge transfer salts.[5,6] However, these data are not adequate to compare with the optimized structures presented above for the DIPS molecule since electron extraction can be expected to induce relevant changes in the geometry of DIPS due to a gain in aromaticity as suggested by Boutique *et al.*[23] In this way, the central C4–C4′ bond is reported to have lengths of 1.429 and 1.435 Å (Refs. 5 and 6), which are considerably longer than that calculated for neutral DIPS in this work (1.375 Å).

Our theoretically optimized geometries should be better compared with the x-ray diffraction structure reported for neutral DIPSΦ_4 (Ref. 38). The experimental parameters observed for the dithiapyranylidene ring are displayed in Fig. 2(b) together with the theoretical geometry obtained for DIPSΦ_4. This geometry has been only optimized at the PM3 level due to the large size of the molecule. As can be observed from Fig. 2(b), the geometric parameters calculated for the DIPS environment are in excellent agreement with the experimental data. When comparing Figs. 2(a) and 2(b), the DIPS ring remains almost unaffected in passing from DIPS to DIPSΦ_4 and only the sulfur environment experiences relevant changes. The C–S bonds lengthen by 0.030 Å to 1.756 Å. Figures 2(a) and 2(b) also show that the PM3 parameters obtained for DIPS [Fig. 2(a)] are in better correlation with the experimental data [Fig. 2(b)] than the STO-3G* parameters [Fig. 2(a)]. For example, the PM3 method predicts bond lengths of 1.375 and 1.342 Å for C4–C4′ and C2–C3 bonds of DIPS, respectively, in very good accord with the experimental values of 1.389 and 1.341 Å reported for DIPSΦ_4, while the STO-3G* method predicts too short lengths (1.356 and 1.325 Å, respectively) for both bonds. These results support the use of the PM3 optimized geometries.

We have not used the x-ray crystallographic structure of DIPSΦ_4 to calculate the electronic properties of this molecule due to the poor description that this structure affords for the phenyl substituents. The phenyl carbon–carbon bond lengths are largely underestimated by the x-ray measurements, since they are reported to be in the range of 1.35 to 1.38 Å. As can be observed from Fig. 2(b), the PM3 method predicts that all the phenyl C–C bonds are of the order of 1.39 to 1.40 Å in accord with the bond distances found in related systems such as biphenyl.[42–44] The phenyl substituents are linked to the central DIPS ring by bonds of 1.472 Å of length in good agreement with the experimental value ($\approx$1.48 Å).[38] This bond length is slightly shorter than that reported for the interannular bond of biphenyl ($\approx$1.50 Å).[42–44]

Finally, it is to be noted that the phenyl rings have been assumed to be coplanar with the central ring of DIPS. Crystallographic data suggest that these rings are twisted by $\approx$10° about the C–C bond to the thiapyranylidene rings.[38] However, this slight deviation from planarity, resulting from the close contact between adjacent hydrogens on DIPS and phenyl rings, does not produce any noticeable effect on the electronic properties calculated for DIPSΦ_4 since, as we will

TABLE I. VEH one-electron energy levels of dithiapyranylidene (DIPS). The molecular orbitals are numbered starting with the lowest-lying valence orbital.

Symmetry	Energy (eV)	Symmetry	Energy (eV)
$1a_g$	− 33.70	$3b_{1g}$	− 16.00
$1b_{3u}$	− 32.11	$4b_{1g}$	− 15.76
$2a_g$	− 29.26	$1b_{1u}$ (π)	− 14.02
$1b_{2u}$	− 29.08	$6a_g$	− 13.74
$1b_{1g}$	− 28.66	$5b_{2u}$	− 13.03
$2b_{3u}$	− 26.39	$1b_{2g}$ (π)	− 13.02
$3a_g$	− 24.68	$6b_{3u}$	− 12.30
$2b_{2u}$	− 23.23	$7a_g$	− 12.23
$3b_{3u}$	− 22.40	$5b_{1g}$	− 11.39
$2b_{1g}$	− 21.14	$2b_{1u}$ (π)	− 11.12
$4a_g$	− 19.83	$1b_{3g}$ (π)	− 10.59
$3b_{2u}$	− 17.85	$1a_u$ (π)	− 10.53
$5a_g$	− 17.62	$2b_{2g}$ (π)	− 9.26
$4b_{3u}$	− 16.81	$3b_{1u}$ (π-HOMO)	− 6.74
$4b_{2u}$	− 16.52	$3b_{2g}$ (π^*-LUMO)	− 4.50
$5b_{3u}$	− 16.42		

see below, the interactions between phenyl and thiapyranylidene rings are very weak. In this way, VEH calculations have been performed over the totally planar D_{2h} geometries of DIPS and DIPSΦ_4 optimized at the PM3 level (Fig. 2).

B. Theoretical XPS spectra

The VEH one-electron energy level distributions calculated for DIPS and DIPSΦ_4 using the PM3 geometries depicted in Fig. 2 are reported in Tables I and II, respectively. The highest occupied molecular orbital (HOMO) corresponds to the 30th MO in the case of DIPS and the 86th in the case of DIPSΦ_4 and shows the same symmetry (b_{1u}) for both systems. The MO distribution obtained for DIPS is very similar to that reported at the STO-3G level,[23] the main difference being the high energy (− 3.55 eV) that the STO-3G basis set predicted for the HOMO level. This energy compares well with that obtained at the STO-3G* level (− 3.57 eV) but overestimates by $\approx$3 eV the energies calculated at the VEH//PM3 (− 6.74 eV) or 4-31G//STO-3G* (− 6.21 eV) double zeta levels. The significance of these differences is discussed below.

In order to facilitate the analysis of the VEH-MO distribution obtained for DIPSΦ_4, this is presented as a convoluted density-of-valence-states (DOVS) spectrum in Fig. 3. The VEH-DOVS spectra calculated for DIPS and benzene are also included in Fig. 3 for the sake of comparison. The spectra in Fig. 3 constitute a theoretical simulation of the photoemission XPS spectra. They have been obtained following the methodology discussed above using a full width at half-maximum of 0.7 eV for the convoluting Gaussian functions and the cross section model of Gelius to modulate

TABLE II. VEH one-electron energy levels of tetraphenyldithiapyranylidene (DIPSΦ_4). The molecular orbitals are numbered starting with the lowest-lying valence orbital.

Symmetry	Energy (eV)	Symmetry	Energy (eV)	Symmetry	Energy (eV)
$1a_g$	− 34.59	$7b_{1g}$	− 20.38	$1a_u$ (π)	− 13.67
$1b_{3u}$	− 34.32	$9a_g$	− 20.21	$14b_{2u}$	− 13.46
$1b_{2u}$	− 34.19	$8b_{2u}$	− 19.35	$2b_{1u}$ (π)	− 13.07
$1b_{1g}$	− 34.18	$9b_{3u}$	− 19.14	$15b_{3u}$	− 12.87
$2a_g$	− 33.24	$8b_{1g}$	− 18.84	$16a_g$	− 12.85
$2b_{3u}$	− 32.02	$10a_g$	− 17.96	$14b_{1g}$	− 12.80
$2b_{2u}$	− 30.31	$9b_{2u}$	− 17.95	$16b_{3u}$	− 12.60
$2b_{1g}$	− 30.12	$11a_g$	− 17.67	$2b_{2g}$ (π)	− 12.51
$3a_g$	− 29.72	$10b_{3u}$	− 17.11	$15b_{2u}$	− 12.33
$3b_{3u}$	− 27.71	$9b_{1g}$	− 17.06	$15b_{1g}$	− 12.21
$4a_g$	− 27.34	$10b_{2u}$	− 16.73	$17a_g$	− 12.21
$3b_{2u}$	− 27.26	$10b_{1g}$	− 16.52	$16b_{2u}$	− 12.03
$4b_{3u}$	− 27.24	$11b_{3u}$	− 16.39	$17b_{3u}$	− 11.53
$3b_{1g}$	− 27.23	$12a_g$	− 16.32	$18a_g$	− 11.47
$5a_g$	− 26.69	$12b_{3u}$	− 16.18	$2b_{3g}$ (π)	− 11.27
$4b_{2u}$	− 26.29	$13a_g$	− 16.03	$2a_u$ (π)	− 11.24
$4b_{1g}$	− 25.98	$11b_{2u}$	− 15.99	$3b_{1u}$ (π)	− 11.22
$5b_{3u}$	− 25.98	$11b_{1g}$	− 15.74	$16b_{1g}$	− 11.17
$6a_g$	− 24.74	$12b_{2u}$	− 15.64	$3b_{2g}$ (π)	− 9.47
$5b_{2u}$	− 23.64	$13b_{3u}$	− 15.63	$4b_{1u}$ (π)	− 9.41
$6b_{3u}$	− 23.35	$14a_g$	− 15.60	$3b_{3g}$ (π)	− 9.39
$5b_{1g}$	− 22.79	$14b_{3u}$	− 15.45	$3a_u$ (π)	− 9.39
$7a_g$	− 22.26	$12b_{1g}$	− 15.44	$4b_{2g}$ (π)	− 9.33
$6b_{2u}$	− 22.10	$13b_{2u}$	− 15.30	$5b_{1u}$ (π)	− 9.31
$6b_{1g}$	− 21.85	$13b_{1g}$	− 14.74	$5b_{2g}$ (π)	− 9.12
$7b_{3u}$	− 21.84	$1b_{1u}$ (π)	− 14.53	$4b_{3g}$ (π)	− 8.53
$8a_g$	− 21.56	$15a_g$	− 14.24	$4a_u$ (π)	− 8.50
$7b_{2u}$	− 21.28	$1b_{2g}$ (π)	− 14.13	$6b_{1u}$ (π HOMO)	− 6.60
$8b_{3u}$	− 20.91	$1b_{3g}$ (π)	− 13.70	$6b_{2g}$ (π^* LUMO)	− 4.87

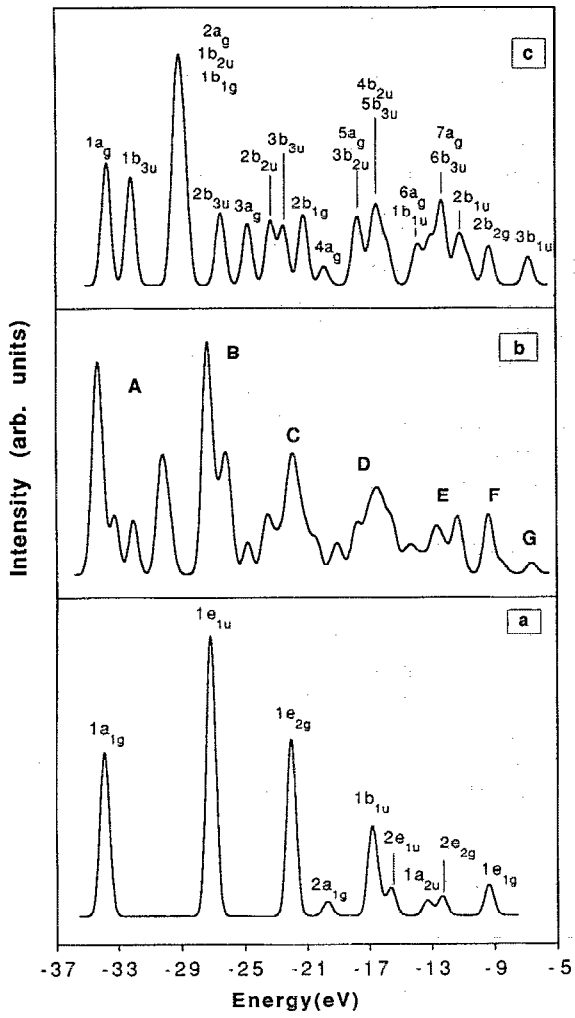

FIG. 3. VEH theoretical simulation of the XPS spectrum for (a) DIPS, (b) DIPSΦ_4, and (c) benzene. The symmetries of the molecular orbitals more significantly contributing to the different peaks are indicated for DIPS and benzene. The molecular orbitals are numbered starting with the lowest-lying valence orbital. Convolutions of the electronic levels are performed by Gaussians with FWHM of 0.7 eV.

TABLE III. VEH energies (eV) corresponding to the most salient features of the valence electronic density of states spectrum displayed in Fig. 3(b) for DIPSΦ_4. The main molecular orbitals (OMs) responsible of each peak structure are indicated in the third column. See Fig. 3(b) for labels.

Structure	Energy	OMs
A	− 34.30	$1a_g$, $1b_{3u}$, $1b_{2u}$, $1b_{1g}$
	− 33.25	$2a_g$
	− 32.00	$2b_{3u}$
	− 30.15	$2b_{2u}$, $2b_{1g}$, $3a_g$
B	− 27.25	$4a_g$, $3b_{2u}$, $4b_{3u}$, $3b_{1g}$
	− 26.10	$4b_{2u}$, $4b_{1g}$, $5b_{3u}$
	− 24.75	$6a_g$
C	− 23.45	$5b_{2u}$, $6b_{3u}$
	− 21.90	$6b_{2u}$, $6b_{1g}$, $7b_{3u}$, $8a_g$
D	− 19.05	$9b_{3u}$, $8b_{1g}$
	− 17.70	$10a_g$, $9b_{2u}$, $11a_g$
	− 16.45	$10b_{2u}$, $10b_{1g}$, $11b_{3u}$
E	− 14.35	$1b_{1u}$, $15a_g$, $1b_{2g}$
	− 12.70	$15b_{3u}$, $16a_g$, $16b_{3u}$, $2b_{2g}$
	− 11.30	$17b_{3u}$, $18a_g$, $3b_{1u}$
F	− 9.35	$3b_{2g}$, $4b_{2g}$, $5b_{1u}$
G	− 6.60	$6b_{1u}$

the intensity of each Gaussian function. The peak structures appearing for DIPSΦ_4 in Fig. 3(b) are identified by labels from A to G. These labels are used in Table III (where the energies of the different peaks are listed for DIPSΦ_4) and in the following discussion. For the benzene molecule, the PM3-optimized geometry ($d_{C\text{-}C} = 1.391$ Å, $d_{C\text{-}H} = 1.095$ Å) has been used in the VEH calculations for the sake of coherence.

We now discuss in detail the atomic origin of each DIPSΦ_4 peak in Fig. 3(b) and the relationships with DIPS or benzene molecular orbitals. Structure A in Fig. 3(b) is formed by four peaks and originates in the 2*s* atomic orbitals of all the carbon atoms and the 3*s* atomic orbitals of sulfur atoms. The analysis of the nine molecular orbitals that give rise to these peaks indicates that the first peak at − 34.30 eV clearly corresponds to the totally bonding $1a_{1g}$ molecular orbital of benzene rings calculated at − 33.90 eV (see Table I in Ref. 48 for a detailed picture of the benzene molecular levels). These orbitals are shifted to lower energies in DIPSΦ_4 due to some bonding interactions with the central ring of DIPS. The shoulder at − 33.25 eV and the small peak at − 32.00 eV result from the C_{2s},S_{3s}–$1a_g$ (totally bonding) and − $1b_{3u}$ (C4–C4′ antibonding) molecular orbitals of DIPS, respectively. Both features are shifted to higher energies in DIPSΦ_4 due to some antibonding interactions with benzene $1a_{1g}$ orbitals. The fourth peak at − 30.15 eV correlates with the third peak of DIPS ($2a_g$, $1b_{2u}$, $1b_{1g}$). These MOs mainly involve bonding interactions in S1–C2, C2–C3, and C4–C4′ bonds and appear at lower energies in DIPSΦ_4 due to some bonding interaction with benzene $1e_{1u}$ levels.

Structure B in Fig. 3(b) is formed by three peaks. The first peak at lower energies corresponds to the most intense peak in the spectrum and originates in the degenerate $1e_{1u}$ molecular orbitals of phenyl rings with no 2*s* contributions on the para carbons. Indeed, this peak appears at − 27.25 eV almost exactly the energy calculated for the $1e_{1u}$ orbitals of benzene (− 27.16 eV). The analysis of the MOs that give rise to the second peak at − 26.10 eV indicates that this peak mainly results from the $2b_{3u}$ molecular orbital of DIPS (S1–C2 and C2–C3 bonds) and the antibonding interaction of the $1b_{1g}$ orbital of DIPS (C2–C3 2*s* bonds) with the $1e_{1u}$ levels of phenyl rings. The small feature at − 24.75 eV comes from

the $3a_g$ molecular orbital of DIPS (C_{2s}, C_{2p_x}, and S_{3s} contributions forming S1–C2, C2–C3, and C4–C4′ bonds).

Peak structures A and B show the largest intensities in the VEH-XPS spectrum due to the fact that they mainly originate in C_{2s} and S_{3s} atomic orbitals which, as discussed in Sec. II, have larger x-ray photoemission cross sections values than C_{2p} and S_{3p} orbitals. This feature determines that the most intense peaks are found in the deepest part of the valence electronic band.

The first peak of structure C at -23.45 eV has an atomic composition mostly due to the DIPS moiety and in particular to the $2b_{2u}$ orbital showing antibonding $C2_{2s}$–$S1_{3s}$ interactions. The second peak at -21.90 eV clearly corresponds to the degenerate C_{2s} $1e_{2g}$ orbitals of phenyl rings (weakly C–H bonding and C–C antibonding) which are calculated at -22.04 eV for the benzene molecule. The structure C also presents a shoulder about -20.40 eV which mainly comes from the $2b_{1g}$ molecular orbital of DIPS shifted to higher energies by some interactions with the $2a_{1g}$ orbitals of phenyl rings.

The atomic composition of the molecular orbitals contributing to the first peak of structure D correlates with the $2a_{1g}$ levels of phenyl rings with a small contribution from the $4a_g$ orbital of DIPS. The low intensity of this peak is due to the fact that both the $2a_{1g}$–benzene and $4a_g$–DIPS orbitals are mainly C_{2p}–H_{1s} bonding. The peak at -17.70 eV is attributed to DIPS since its orbital composition indicates contributions from the $3b_{2u}$ (strongly C_{2p}–C_{2p} and C_{2p}–S_{3p} bonding) and $5a_g$ (strongly C_{2s}–H_{1s} bonding, C_{2s}–C_{2s} and C_{2s}–S_{3s} antibonding) MOs of DIPS. Although as many as 16 one-electron levels contribute to the rest of structure D, the main peak at -16.45 eV can be clearly correlated with the C_{2s} $1b_{1u}$ molecular orbitals of benzene moieties (strongly C_{2s}–H_{1s} bonding and C_{2s}–C_{2s} antibonding). The shoulder about -15.75 eV mainly derives from the strongly C_{2p}–H_{1s} bonding $2e_{1u}$ orbitals of phenyl rings.

We now turn to the analysis of the outer part of the valence electronic structure of DIPSΦ_4. As many as 23 molecular orbitals are involved in the broad peak structure E, 9 of which are of π nature. The first peak at -14.35 eV is a mixture of σ and π contributions and mainly results from the totally bonding $1b_{1u}$ (π) and the weakly C_{2p}–C_{2p} bonding $6a_g(\sigma)$ molecular orbitals of DIPS. The second peak at -12.70 eV is of σ nature and mostly originates in the $6b_{3u}$ and $7a_g$ orbitals of DIPS with some contribution from benzene $2e_{2g}$ levels. The third peak at -11.30 eV is again a mixture of σ and π character and mainly results from DIPS. The first two orbitals ($17b_{3u}$ and $18a_g$) contributing to this peak have strong contributions from S_{3s} and S_{3p_x} atomic orbitals and clearly correspond to the σ-lone pairs of sulfur atoms. The rest of the orbitals about -11.20 eV are of π nature and are mainly localized on the central ring of DIPS.

Structure F involves an unique peak located at -9.35 eV. The nine orbitals contributing to this peak are of π nature and have the same atomic composition as the degenerate $1e_{1g}$ π orbitals of benzene (-9.37 eV) with small contributions from the $2b_{2g}$ π orbital of DIPS. Finally, the small peak G at -6.60 eV is only due to the $6b_{1u}$ highest occupied molecular orbital of DIPSΦ_4 which lies alone 1.9 eV above

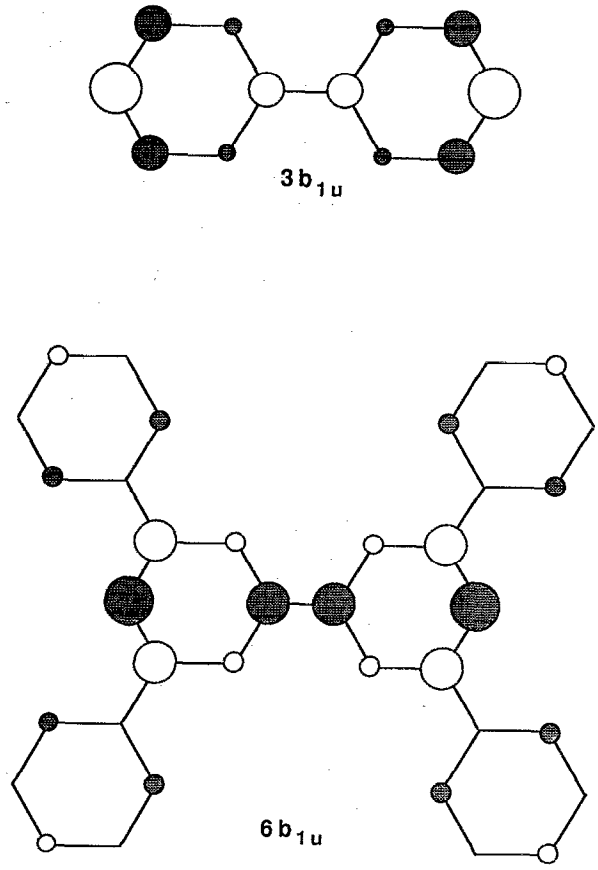

FIG. 4. Atomic orbital (AO) composition of the $3b_{1u}$ and $6b_{1u}$ highest occupied molecular orbitals of DIPS (upper) and DIPSΦ_4 (lower), respectively. The size of the circles is approximately proportional to the magnitude of the AO coefficients. A white area indicates a positive value for the upper lobe of the p_π-AO, while a grey area indicates a negative value.

the following occupied orbital. The atomic composition of this molecular orbital is sketched in Fig. 4 together with that of the $3b_{1u}$ HOMO of DIPS. When comparing both molecular orbitals, it becomes clear that peak G originates in the $3b_{1u}$ HOMO of DIPS. This orbital reflects the alternating double bond structure present in DIPS and DIPSΦ_4 since it shows bonding interactions between atoms forming double bonds, C4–C4′ and C2–C3 (less intense), and antibonding interactions between atoms forming single bonds, S1–C2 and C3–C4 (less intense).

The preceding analysis shows that the characteristics of the electronic structure of both the central ring of DIPS and the phenyl substituents are mostly conserved in the DIPSΦ_4 molecule and a simple correlation between the one-electron energy levels of DIPS and benzene molecules and those of DIPSΦ_4 can be established. Thus we have to conclude that, from a electronic structure standpoint, DIPSΦ_4 results from the superposition of the electronic structures of its molecular components DIPS and benzene. This result contrasts with those obtained by El-Khatib *et al.*[21,22] who suggested that it was not possible to obtain the main features of the eigenvalue spectrum of DIPSΦ_4 from calculations on smaller model molecules. Furthermore, the Xα calculations performed by

these authors predict a phenyl character for the HOMO of DIPSΦ_4 in contrast with the DIPS character obtained in our VEH calculations. The increase in the energy of the HOMO these authors obtain when passing from DIPSΦ_4 (-12.57 eV) to DIPS (-10.09 eV) is not understandable if the HOMO level mainly originates in phenyl rings as they suggest.[21,22] Our predictions are supported by the almost identical oxidation potentials measured for DIPS (0.20 V) and DIPSΦ_4 (0.22 V) vs SCE (standard calomel electrode) in CH_2Cl_2 solvent.[18(b)] Since oxidation implies removing an electron from the HOMO, it is reasonable to expect that molecules with similar oxidation potentials have HOMOs lying at similar energies as we predict for DIPS and DIPSΦ_4.

The lowest unoccupied molecular orbital (LUMO) of DIPSΦ_4 corresponds to the $6b_{2g}$ π^* level. This orbital is calculated at -4.87 eV and is mainly located on the central ring of DIPS. Indeed, it shows an atomic composition similar to that displayed for the HOMO in Fig. 4 but now bonding interactions only take place on C3–C4 single bonds. For the DIPS molecule, the LUMO corresponds to the $3b_{2g}$ π^* level and lies at -4.50 eV. The HOMO-LUMO gap obtained from our VEH calculations has a value of 1.73 eV for DIPSΦ_4 in quite good agreement with the experimental gap of 2.03 eV measured from optical data.[22] The theoretical gap increases when passing to DIPS (2.24 eV) as experimentally observed for different series of dichalcogenapyrans.[4,17,18]

C. Correlation with experimental XPS spectra

In Fig. 5, we compare the VEH-DOVS spectrum calculated for DIPSΦ_4 with the solid-state XPS spectrum reported by Boutique *et al.*[20] To make properly the comparison between theory and experiment, the theoretical spectrum has been contracted along the energy scale in order to correct for the too wide valence band that Hartree–Fock *ab initio* calculations and, therefore, VEH calculations provide. A consistent value of 1.3 has been used for the contraction factor as in almost all the comparisons which have been previously made between VEH calculated and experimental photoemission spectra.[1–3,48,49] Since theoretical calculations are performed on isolated molecules, the theoretical spectrum should be also shifted to lower binding energies to take into account the polarization energy due to solid-state relaxation effects. In this way, a rigid shift of 5.35 eV has been applied to the VEH spectrum in order to align the theoretical peak F calculated at 9.35 eV with the second XPS peak located at 4.0 eV (Ref. 20). However, if we consider that theoretical binding energies are referred to the vacuum level while experimental energies are measured relative to the Fermi level, and that, as discussed below, the theoretical and experimental features aligned correspond to the $1e_{1g}$ HOMO levels of benzene for which a value of 4.1 eV is estimated for its work function,[50] we are actually applying a shift of only 1.25 eV $\{9.35-(4.0+4.1)\}$ to the theoretical spectrum. This energy value represents an approximated estimate of the solid-state polarization energy. The binding energies and atomic composition of the most salient features of the theoretical and experimental XPS spectra are collected in Table IV to facilitate the analysis of the correspondence between theory and experiment.

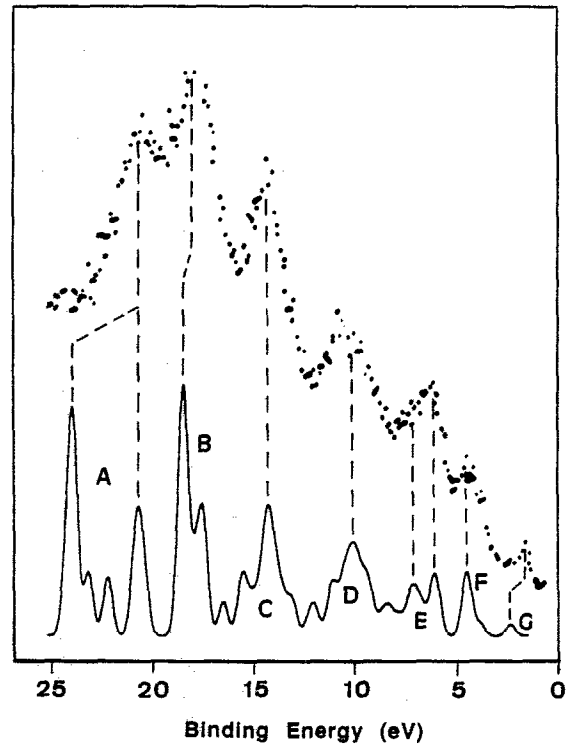

FIG. 5. Comparison of theoretical VEH (lower curve) and experimental (upper curve) XPS spectra for tetraphenyldithiapyranylidene (DIPSΦ_4). The theoretical spectrum is contracted and shifted as discussed in the text. Gaussians with FWMH of 0.7 eV are used in the convolution process. Labels correspond to those displayed in Fig. 3(b). The experimental spectrum is taken from Ref. 20.

As can be seen from Fig. 5 and Table IV, the overall agreement between the theoretical and experimental spectra is very good. We have chosen peak F to perform the fitting between the theoretical and experimental XPS spectra because this peak has been unambiguously assigned to the $1e_{1g}$ π orbitals of the four phenyl rings. On the other hand and from a purely experimental standpoint, the XPS peak at 4.0 eV appears at almost the same binding energy than that reported for the $1e_{1g}$ HOMO levels of benzene (3.85 eV) from its solid-state XPS spectrum.[50] Finally, it should be remembered that VEH calculations predict a binding energy of 9.37 eV for the $1e_{1g}$ orbitals of benzene in perfect accord with the reported gas-phase UPS value of 9.4 eV (Ref. 51). Therefore, the XPS peak at 4.0 eV must be clearly aligned with theoretical peak F, as performed in Fig. 5 and Table IV.

The few intense photoemission bands observed in the experimental XPS spectrum at a binding energy of only 1.2 eV is to be correlated with the theoretical peak G calculated at 1.89 eV. As discussed above, this peak results from the $6b_{1u}$ HOMO of DIPSΦ_4 and can be considered as an intrinsic feature of the central ring of DIPS. VEH calculations overestimate the binding energy of this peak by 0.7 eV because a double-zeta basis set is not diffuse enough to adequately reproduce the sulfur lone pair contributions. The

TABLE IV. Calculated (VEH) and measured (XPS) binding energies (eV) for the most salient features of the valence electronic structure of tetraphenyldithiapyranylidene (DIPSΦ_4).

Feature[a]	VEH[b]	VEH[c]	XPS[d]	XPS[e]
A (C_{2s}, $1a_{1g}$)	34.30	23.19		
(S_{3s}, C_{2s} DIPS)	30.15	20.0	20.2	20.4
B (C_{2s}, $1e_{1u}$)	27.25	17.77	17.5	17.27
(S_{3s}, C_{2s} DIPS)	26.10	16.89		
C (S_{3s}, C_{2s} DIPS)	23.45	14.85		
(C_{2s}, $1e_{2g}$)	21.90	13.65	13.9	13.65
D (C_{2p}–H_{1s}, $2a_{1g}$)	19.10	11.50	10.4	
(C_{2p}, S_{3p} DIPS)	17.70	10.42		
(C_{2s}–H_{1s}, $1b_{1u}$)	16.45	9.46	9.4	9.65
E (C_{2p}, S_{3p} DIPS)	12.70	6.58	6.8 (sh)[f]	7.27
($S_{2s,3p}$ σ-lone pairs)	11.30	5.50	5.8	
F (C_{2p}, $1e_{1g}$ π)	9.35	4.0	4.0	3.9
G ($3b_{1u}$ π-MO, DIPS)	6.60	1.89	1.2	1.25

[a] Labels correspond to those displayed in Figs. 3(b) and 5. The main atomic contributions are indicated in parentheses according to Sec. III B. Contributions from the phenyl rings are denoted by the symmetry labels of the corresponding MOs of benzene.
[b] VEH binding energies calculated using Koopmans' theorem.
[c] VEH binding energies after contraction of 1.3 of the energy scale and a rigid shift of the valence band to match the second experimental feature at 4.0 eV.
[d] Experimental binding energies from the solid-state XPS spectra reported in Ref. 20. Energies are referred to the Fermi level.
[e] Experimental bindings from solid-state XPS spectra reported in Ref. 22. Energies are referred to the Fermi level.
[f] sh denotes a shoulder.

low energy of this peak originates in the strong antibonding interaction that takes place between the sulfur atoms and the adjacent carbons atoms (see Fig. 4). This antibonding interactions unstabilize the $6b_{1u}$ π HOMO of DIPSΦ_4 and are not observed in other related heterocycles like thiophene, for which a higher first ionization energy is measured (8.85 eV referred to the vacuum level).[52]

Previously reported minimal STO-3G basis set calculations[23] located the HOMO level of the DIPS molecule at -3.55 eV. This energy is $\approx$3.1 eV higher than those obtained in this work for DIPS (-6.74 eV) or DIPSΦ_4 (-6.60 eV) using the VEH method and is in clear disagreement with the experimental XPS data since it would imply a too small first ionization potential for DIPSΦ_4. This is not an unexpected result since the STO-3G basis set also predicts very small ionization potentials for related molecules like thiophene (6.85 eV) and it is a necessary requirement to use at least a double-zeta basis set to obtain acceptable estimates (9.31 eV with a 3–21 G basis set) of the experimental ionization potential (8.85 eV).[52]

Boutique *et al.*[20] report that the third photoemission band of the experimental XPS spectrum consists of a main peak at 5.8 eV, which broadens on its high binding energy side showing a shoulder at 6.8 eV. This is exactly the structure observed for the theoretical band E which presents a peak at 5.5 eV followed by a less intense peak at 6.6 eV. As discussed in Sec. III B, peak structure E mainly derives from DIPS, the first peak coming from sulfur σ-lone pairs and the second peak originating in S_{3p}–C_{2p} σ bonding. The relative high intensity of both peaks is due to the strong contributions from sulfur $3s$ and $3p$ atomic orbitals.

The broad experimental band centered between 9 and 11 eV perfectly correlates with the theoretical structure D. In contrast with El-Khatib *et al.*[21,22] that report an unique peak centered at 9.65 eV, Boutique *et al.*[20] predict the existence of two-well differentiated peaks at 9.4 and 10.4 eV. The first of these peaks is in excellent correlation with the main peak of structure D calculated at 9.46 eV. This peak is localized within the four phenyl rings of DIPSΦ_4 since it results from the $1b_{1u}$ orbital of benzene. The second peak at 10.4 eV has no clear correspondence in the theoretical spectrum and could be, in principle, associated with the shoulder that structure D presents at 10.42 eV. The experimental peak could also involve contributions from the small peak calculated at 11.50 eV since the benzene $2a_{1g}$ orbitals that give rise to this peak are calculated 0.7 eV too high in binding energy for other systems containing phenyl substituents like polystyrene.[48] In a similar way to DIPSΦ_4, polystyrene presents a photoemission band centered at 9.5 eV with a shoulder about 10.5 eV which are attributed to benzene $1b_{1u}$ and $2a_{1g}$ levels, respectively.[48]

We now turn to discuss the inner part of the valence XPS spectrum of DIPSΦ_4 which is dominated by carbon $2s$ and sulfur $3s$ contributions. The experimental band at 13.9 eV (13.65 eV from El-Khatib *et al.*[22]) clearly correlates with the theoretical structure C whose main peak is calculated at 13.65 eV and has been assigned to the C_{2s} $1e_{2g}$ orbitals of benzene moieties. Indeed, these orbitals are reported to appear at 13.6 eV in the solid-state XPS spectrum of benzene.[50] Theoretical structure C shows a peak on its higher binding energy side (14.85 eV) that results from DIPS and is not clearly observed in the experimental spectrum.

The most intense photoemission band is measured to be centered about 17.5 eV and can be associated with the theoretical structure B. The main peak of this structure is localized again on the four phenyl rings (C_{2s} $1e_{1u}$ orbitals) and is predicted 0.3 eV too high in binding energy by the VEH method (see Table IV) in the same way that was previously reported for the benzene molecule.[48]

Finally, the XPS band at 20.2–20.4 eV is correlated with the theoretical peak structure A. This structure mainly consists of two intense peaks calculated at 23.2 and 20.0 eV. The peak at 20.0 eV is in good correlation with the experimental band and it mostly results from S_{3s} and C_{2s} contributions from the central ring of DIPS. The peak at 23.2 eV corresponds to the totally bonding C_{2s} $1a_{1g}$ orbitals of phenyl rings which, as previously discussed,[1,48] are calculated by the VEH method to lie about 2.2–2.4 eV too high in binding energy. This is an expected result since the VEH method is parameterized to reproduce the outer part of the valence band and the lowest-lying levels are calculated to be too low in energy, especially for hydrocarbons.[48] We think therefore

that the $1a_{1g}$ peak, located about 20.8–21.0 eV after subtracting the 2.2–2.4 factor, also contributes to the highest binding energy valence photoemission band.

In summary, we can say that the VEH-DOVS-XPS spectrum calculated for the DIPSΦ_4 molecule is fully consistent with the solid-state XPS spectrum of Boutique *et al.* and allows for a complete interpretation of the experimental photoemission bands.

IV. SUMMARY AND CONCLUSIONS

We have investigated the electronic structure of the tetraphenyldithiapyranylidene (DIPSΦ_4) π-donor molecule using the valence effective Hamiltonian (VEH) nonempirical technique. Theoretical calculations have been performed on PM3 optimized geometries which suggest that DIPSΦ_4 is essentially a nonaromatic system since single and double bonds alternate in the central ring of dithiapyranylidene (DIPS). The electronic structure of DIPSΦ_4 presented as convoluted DOVS curves has been analyzed in every detail and a one-to-one correspondence has been established between the electronic peak structures that constitute the DOVS curves of DIPSΦ_4 and the one-electron energy levels calculated for its molecular components DIPS and benzene. We have therefore to conclude that the electronic characteristics of DIPS and benzene moieties are preserved in the DIPSΦ_4 molecule and that, both from the structural and the electronic standpoints, DIPSΦ_4 must be viewed as the result of adding the geometrical and the electronic structures of its molecular components, respectively.

The VEH-DOVS curves convoluted to simulate the XPS spectrum have been compared with the experimental solid-state XPS spectrum reported by Boutique *et al.*[20] for DIPSΦ_4. The theoretical curves are fully consistent with the solid-state spectrum and an excellent quantitative agreement between theory and experiment is found when comparing the positions and intensities of the main peaks. A complete interpretation of all features appearing in the XPS spectrum has been performed in the light of VEH predictions which allow us to disentangle the atomic parentage of each experimental photoemission band. The VEH-based assignments are in perfect agreement with those previously suggested on a purely experimental basis[20] and contrast with those performed on the basis of Xα calculations.[21,22]

ACKNOWLEDGMENTS

The authors acknowledge stimulating discussions with Professor J. L. Brédas. They thank the CIUV (Centro de Informática de la Universitat de València) for the use of their computing facilities. This work has been supported by the DGICYT Project Nos. PS88-0112 and OP90-0042 and the CICYT Project No. MAT88-0239.

[1] E. Ortí and J. L. Brédas, J. Chem. Phys. **89**, 1009 (1988).
[2] E. Ortí and J. L. Brédas, J. Am. Chem. Soc. (submitted).
[3] E. Ortí and J. L. Brédas, Chem. Phys. Lett. **164**, 247 (1989).
[4] D. J. Sandman, A. J. Epstein, T. J. Holmes, and A. P. Fisher III, J. Chem. Soc., Chem. Commun. 177 (1977).
[5] B. F. Darocha, D. D. Titus, and D. J. Sandman, Acta Crystallogr. B **35**, 2445 (1979).
[6] D. J. Sandman, A. J. Epstein, T. J. Holmes, J. S. Lee, and D. D. Titus, J. Chem. Soc. Perkin Trans. 2, 1578 (1980).
[7] J. Alizon, J. Blanc, J. Gallice, H. Robert, C. Fabre, H. Strzelecka, J. Rivory, and C. Weyl, in *Lecture Notes in Physics, 65: Organic Conductors and Semiconductors*, edited by L Pal, G. Grüner, A. Janossy, and J. Solyom (Springer, New York, 1977), pp. 563–569; J. H. Perlstein, Angew. Chem. Int. Ed. Engl. **16**, 519 (1977).
[8] H. Strzelecka, W. Schoenfelder, and J. Rivory, Mol. Cryst. Liq. Cryst. **52**, 307 (1979).
[9] L. C. Isset, G. A. Reynolds, E. D. Schneider, and J. H. Perlstein, Solid State Commun. **30**, 1 (1979).
[10] H. Strzelecka and J. Rivory, Mat. Res. Bull. **15**, 899 (1980); D. Chasseau, J. Gaultier, C. Hauw, S. Lefrant, J. Rivory, E. Rzepka, and H. Strzelecka, Solid State Commun. **34**, 873 (1980); V. Gionis, R. Fugnitto, G. Mayer, H. Strzelecka, and J. C. Dubois, Mol. Cryst. Liq. Cryst. **90**, 153 (1982).
[11] P. A. Albouy, J. P. Pouget, and H. Strzelecka, Phys. Rev. B **35**, 173 (1987).
[12] E. Faulques, E. Rzepka, S. Lefrant, and H. Strzelecka, Mol. Cryst. Liq. Cryst. **86**, 63 (1982); C. Garrigou-Lagrange and H. Strzelecka, J. Chim. Phys. **87**, 1763 (1990).
[13] M. Maitrot, G. Guillaud, B. Boudjema, J. J. André, H. Strzelecka, J. Simon, and R. Even, Chem. Phys. Lett. **133**, 59 (1987).
[14] N. El-Khatib, B. Boudjema, G. Guillaud, M. Maitrot, and H. Chermette, J. Less-Common Met. **143**, 101 (1988).
[15] H. Strzelecka, R. Vicente, J. Ribas, J.-P. Legros, P. Cassoux, P. Petit, and J.-J. André, Polihedron **10**, 687 (1991).
[16] C. H. Chen and G. A. Reynolds, J. Org. Chem. **45**, 2448, 2453, 2458 (1980); G. A. Reynolds and C. H. Chen, J. Heterocycl. Chem. **18**, 1235 (1981); C. H. Chen, J. J. Doney, and G. A. Reynolds, J. Org. Chem. **47**, 680 (1982); K. Kakasizi, M. Nakatsuka, and I. Murata, J. Chem. Soc., Chem. Commun. 1143 (1981); D. J. Sandman, F. J. Holmes, and D. E. Warner, J. Org. Chem. **44**, 880 (1979).
[17] S. Es-Seddiki, G. LeCoustumer, and Y. Mollier, Tetrahedron Lett. 2771 (1981).
[18] (a) M. R. Detty and B. J. Murray, J. Org. Chem. **47**, 1147 (1982); (b) M. R. Detty, B. J. Murray, and J. H. Perlstein, Tetrahedron Lett. 539 (1983).
[19] M. R. Detty, J. W. Hasset, B. J. Murray, and G. A. Reynolds, Tetrahedron **41**, 4853 (1985).
[20] J. P. Boutique, J, Riga, J. J. Verbist, H. Strzelecka, and J. Rivory, Chem. Phys. **67**, 355 (1982).
[21] N. El-Khatib, M. Maitrot, H. Chermette, L. Porte, and H. Strzelecka, J. Chim. Phys. **84**, 839 (1987).
[22] N. El-Khatib, H. Chermette, and M. Maitrot, Int. J. Quantum Chem. **35**, 339 (1989).
[23] J. P. Boutique, J. J. Verbist, J. G. Fripiat, and J. Delhalle, J. Chem. Soc. Perkin Trans. 2, 239 (1984).
[24] E. Ortí, J. L. Brédas, and C. Clarisse, J. Chem. Phys. **92**, 1228 (1990).
[25] E. Ortí, M. C. Piqueras, R. Crespo, and J. L. Brédas, Chem. Mater. **2**, 110 (1990).
[26] G. Nicolas and Ph. Durand, J. Chem. Phys. **70**, 2020 (1979); **72**, 453 (1980).
[27] J. M. Andre, L. A. Burke, J. Delhalle, G. Nicolas, and Ph. Durand, Int. J. Quantum Chem. Symp. **13**, 283 (1979).
[28] J. L. Brédas. R. R. Chance, R. Silbey, G. Nicolas, and Ph. Durand, J. Chem. Phys. **75**, 255 (1981).
[29] J. L. Brédas, B. Thémans, and J. M. André, J. Chem. Phys. **78**, 6137 (1983).
[30] J. L. Brédas. R. R. Chance, R. Silbey, G. Nicolas, and Ph. Durand, J. Chem. Phys. **77**, 371 (1982).
[31] V. Gelius, in *Electronic Spectroscopy*, edited by D. A. Shirley (North-Holland, Amsterdam, 1972), p. 311.
[32] M. R. Peterson and R. A. Poirier, Department of Chemistry, Toronto University, Ontario, M55 1A1, Canada.
[33] C. J. Marsden and B. J. Smith, J. Mol. Struct., Theochem **105**, 383 (1983); G. Schultz, I. Hargittai, and P. Friedman, J. Mol. Struct. **176**, 61 (1988); W. J. Hehre, L. Radom, P. v. R. Schleyer, and J. A. Pople, *Ab Initio Molecular Orbital Theory* (Wiley, New York, 1986), Chap. 6, p. 135.
[34] J. J. P. Stewart, J. Comput. Chem. **10**, 209, 221 (1989).
[35] J. J. P. Stewart, MOPAC: *A General Molecular Orbital Package* (Version 6.0), Q.C.P.E. 455, **10** (1990).
[36] M. J. S. Dewar and W. Thiel, J. Am. Chem. Soc. **99**, 4899 (1977).
[37] M. J. S. Dewar, E. G. Zoebisch, E. F. Healy, and J. J. P. Stewart, J. Am. Chem. Soc. **107**, 3902 (1985).

[38] H. R. Luss and D. L. Smith, Acta Crystallogr. B **36**, 986 (1980).
[39] J. N. MacDonald, S. A. Mackay, J. K. Tyler, A. P. Cox, and I. C. Ewart, J. Chem. Soc. Faraday Trans. 2 **77**, 79 (1981).
[40] B. P. Stoicheff and J. M. Dowling, Can. J. Phys. **37**, 703 (1959).
[41] L. H. Scharpen and V. W. Laurie, J. Chem. Phys. **43**, 2765 (1965).
[42] G. Häfelinger and C. Regelmann, J. Comput. Chem. **8**, 1057 (1987).
[43] G. B. Robertson, Nature (London) **191**, 593 (1961).
[44] S. Tsuzuki and K. Tanabe, J. Phys. Chem. **95**, 139 (1991).
[45] B. Bak, D. Christensen, W. B. Dixon, L. Hansen-Nygaard, J. Rastrup-Andersen, and M. Schottländer, J. Mol. Spectrosc. **18**, 344 (1965).
[46] M. J. S. Dewar and M. L. Mckee, J. Comput. Chem. **4**, 4 (1983).
[47] J. J. P. Stewart, J. Computer-Aided Mol. Design **4**, 1 (1990).
[48] E. Ortí, J. L. Brédas, J. J. Pireaux, and N. Ishihara, J. Electron Spectrosc. Relat. Phenom. **52**, 551 (1990).
[49] J. L. Brédas and W. R. Salaneck, J. Chem. Phys. **85**, 2219 (1986); S. P. Kowlaczyk, S. Stafström, J. L. Brédas, W. R. Salaneck, and J. L. Jordan-Sweet, Phys. Rev. B **41**, 1645 (1990).
[50] J. Riga, J. J. Pireaux, and J. J. Verbist, Mol. Phys. **34**, 131 (1977).
[51] M. I. Al-Joboury and D. W. Turner, J. Chem. Soc. 4434 (1964).
[52] L. Klasinc, A. Sabljic, G. Kluge, J. Rieger, and M. Scholz, J. Chem. Soc., Perkin Trans. 2, 539 (1982).